International Journal of Electrical and Computer Engineering (IJECE)
Vol. 16, No. 1, February 2026, pp. 414~422
ISSN: 2088-8708, DOI: 10.11591/ijece.v16i1.pp414-422

Deep learning architecture for detection of fetal heart anomalies

Nusrat Jawed Iqbal Ansari[1,2], Maniroja M. Edinburgh[1], Nikita[3]
[1]Department of Electronics and Telecommunication Engineering, Thadomal Shahani Engineering College, Mumbai, India
[2]Department of Computer Engineering, Vivekanand Education Society's Institute of Technology, Mumbai, India
[3]Certified Gynecologist and Fetal Medicine Specialist, P.G. Medical Trust Hospital, Kerala, India

Article Info

Article history:

Received Mar 4, 2025
Revised Oct 4, 2025
Accepted Nov 23, 2025

Keywords:

Augmentation
Deep learning
Echocardiography
Generative adversarial networks
Prenatal

ABSTRACT

Research has demonstrated that artificial intelligence (AI) techniques have shown tremendous potential over the past decade for analyzing and detecting anomalies in the fetal heart during ultrasound tests. Despite their potential, the adoption of these algorithms remains limited due to concerns over patient privacy, the scarcity of large well-annotated datasets and challenges in achieving high accuracy. This research aims to overcome these limitations by proposing an optimal solution. Two methods such as deterministic image augmentation techniques and Wasserstein generative adversarial network with gradient penalty (WGAN-GP) showcase the framework's capacity to seamlessly and effectively expand original datasets to 14 times and 17 times respectively, thereby effectively tackling the problem of data scarcity. It uses an annotation tool to precisely categorize anomalies identified in the echocardiogram dataset. Segmentation of the annotated data is done to highlight region of interest. Nine distinct fetal heart anomalies are identified with respect to the fewer covered in existing research. This study also investigates the state-of-the-art architectures and optimization techniques used in deep learning models. The results clearly indicate that the ResNet-101 model demonstrated superior precision accuracy of 99.15%. To ensure the reliability of the proposed model, its performance underwent thorough evaluation and validation by certified gynecologists and fetal medicine specialists.

Corresponding Author:

Nusrat Jawed Iqbal Ansari
Department of Electronics and Telecommunication Engineering, Thadomal Shahani Engineering College
Mumbai, India
Department of Computer Engineering, Vivekanand Education Society's Institute of Technology
Mumbai, India
Email: nusrat.ansari@ves.ac.in

1. INTRODUCTION

Fetal heart anomalies encompass a wide spectrum of structural and functional disorder, from relatively simple defects such as septal abnormalities to complex congenital malformations like hypoplastic left heart from the left syndrome and transposition of the great arteries. Early and precise identification through prenatal ultrasound is essential, ensuring diagnoses align with standardized protocols. Guidelines established by the International Society of Ultrasound in Obstetrics and Gynecology (ISUOG) offer a structured approach to fetal cardiac assessment, promoting consistency in clinical practice [1]. The American Institute of Ultrasound in Medicine (AIUM) highlights that fetal echocardiography focuses on the evaluation of the fetal heart using ultrasound imaging, which is recognized as reliable, secure and non-invasive [2]. However, healthcare professionals encounter obstacles related to fetal heart abnormalities, such as constraints in ultrasound resolution, variability in fetal positioning, gestational age-dependent visibility of cardiac

structures and limited diagnostic capabilities in certain regions [3]. Deep learning (DL) plays a crucial role in medical imaging by enabling automated image segmentation, helping to identify and isolate fetal heart structures for precise analysis. It enhances classification, improves image reconstruction. Through image synthesis, it generates high-quality synthetic fetal heart images for training and research [4], [5]. In medical imaging, deep learning models often face challenges due to the limited availability of annotated datasets. This scarcity can lead to overfitting [6] where models fail to generalize to new unseen data [7]. Additionally, small datasets may not capture the full variability of medical conditions, limiting the model's robustness and diagnostic accuracy. For sensitive healthcare domain, synthetic data can be used to artificially increase the size of training datasets and it can help deep learning models become more adaptable, reliable, and resilient to variations [8]. Multi-task deep learning applications have achieved significant success in fetal heart assessments, aiding in the detection of neonatal conditions from ultrasound scans [9]–[12]. The existing research [13] introduces a domain-specific data augmentation strategy for medical imaging tasks. It demonstrates how context-preserving augmentation can enhance model performance in fetal ultrasound classification. Miskeen *et al.* [14] highlights extensive investigation of several methods for identifying prenatal heart disease. Nowak *et al.* [15] provides a systematic strategy to ultrasound data augmentation with the goal of improving classification performance for fetal standard plane detection. It emphasizes the importance of optimal augmentation procedures in medical images. Balaha *et al.* [16] investigates several data augmentation and preprocessing strategies for improving deep learning models for medical applications. The findings show that rotation is the most successful augmentation approach, increasing in-domain accuracy by 10.1%. Tiago *et al.* [17] focuses on improving X-ray categorization for necrotizing enterocolitis (NEC), an uncommon but dangerous infant illness. Due to scarcity of images, the authors examined how various image adjustments and preparation techniques can overcome data scarcity and artificial intelligence (AI) models' ability for better detection [18], [19].

This research addresses the challenge of data scarcity in the study of fetal heart abnormalities. Although this area has been extensively explored, it was found that relatively little work had been dedicated to enhancing model training through data augmentation techniques, particularly those based on Wasserstein generative adversarial networks with gradient penalty (WGAN-GP) and deterministic image augmentation. Using deterministic image augmentation, two augmentation levels were applied, expanding the original datasets around 14 times and around 17 times using WGAN-GP. With this enlarged dataset, the deep learning model achieved higher accuracy and able to detect five complex congenital heart anomalies: hypoplastic heart syndrome (HLHS), transposition of the great arteries (TGA), aberrant right subclavian artery (ARSA), echogenic intracardiac focus (ECIF), and dilated cardiac sinus (DCS) within a single study. This advancement enhances the model's utility for medical professionals in fetal cardiac assessment. ResNet-101 was selected for its ability to address the gradient loss issue and deliver optimal results. Prior to utilizing ResNet-101, echocardiography images were examined using several other models, including ResNet-50, DenseNet169, VGG16, and EfficientNetB0. However, the results were unsatisfactory. Therefore, the transition to ResNet-101, coupled with deterministic and WGAN-GP augmentation, yielded significantly improved outcomes. Also, six out of nine classes achieved full performance accuracy using ResNet-101.

The structure of this paper is as follows: Section 2 elaborates on proposed model adopted for artifacts development. Section 3 discuss the result that compare the proposed framework's outcomes to earlier studies, highlighting the effectiveness of the chosen techniques in achieving accurate disease diagnosis with minimum data. Section 4 concludes the paper and future scope of this work.

2. METHOD

2.1. Conceptual diagram

The comprehensive workflow for the proposed system is shown in Figure 1. It consists of the following steps:

a. Data preparation: The most sighted data was selected, followed by data cleaning and preprocessing on the chosen images
b. Defect identification: Under the supervision of experts, each defect was given a name and labelled using *LabelMe* in Anaconda.
c. The segmentation technique involves partitioning an image into distinct regions to effectively identify the region of interest (ROI), which is crucial for precise analysis and interpretation.
d. The implementation and assessment of deep learning algorithms for data analysis

2.2. Dataset

In this research, openly accessible dataset fetal echocardiography (FECG) was used [20]. Thirteen structures have been identified namely left ventricular outflow tract (LVOT), right ventricle (RV), left ventricle (LV), aorta (Ao), right atrium (RA), left atrium (LA), right ventricle (RV), left ventricle (LV), right

hypoplastic heart syndrome (HLHS), atrial septal defect (ASD), ventricular septal defect (VSD), transposition of the great arteries (TGA), normal heart (NH), Dilated Cardiac Sinus (DCS) and echogenic intracardiac focus (ECIF). Subsequently, Certified Gynecologist and Fetal Medicine Specialist examined each individual image that was taken from the FECG recordings and recommended that the higher sighted images to be taken into consideration. The raw, unstructured data was organized and normalized to improve quality, consistency, and reduce redundancy. Normalization included removing duplicates, standardizing formats, handling missing values, and scaling numerical features. These preprocessing tasks ensured the data was clean, consistent, and ready for analysis The pixels are normalized as per given equation.

$$x` = \frac{x.W}{w} \; and \; y` = \frac{y.H}{h} \tag{1}$$

where (x, y) are original coordinates, $(x`, y`)$ are new coordinated after resizing and (w, h) are the original width and height of the image and W, H are new width and height of the image.

$$Normalizing\ pixel\ value: I_{normalized}(x, y) = \frac{I_{(x,y)}}{255} \tag{2}$$

For RGB images, each channel is normalized as:

$$I_{normalized}(c, x, y) = \frac{I_{(c,x,y)} - \mu_c}{\sigma_c} \tag{3}$$

where $I(c, x, y)$ is the pixel intensity at channel c and σ_c and μ_c are the standard deviation and mean of the channel c.

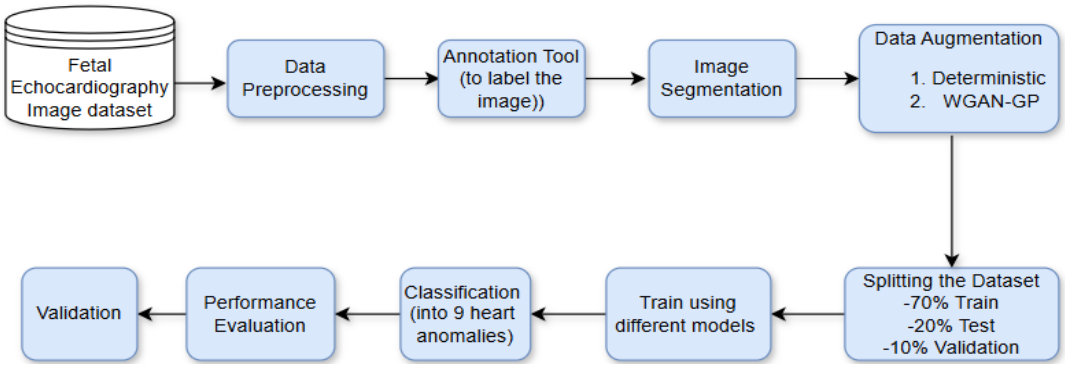

Figure 1. Functional architecture and interrelations within the system

The distribution of echocardiogram data for performance evaluation is seen in Table 1. The procedure for segmenting relies on the anatomical structures of the heart. Using the data labeling tool LabelMe, exact boundaries are drawn around the heart images which will spot the precise position of anomalies. Table 2 gives an illustration of a feature map derived from LabelMe and segmentation.

Table 1. Original dataset summary without augmentation

Class	Training	Testing	Validation	Tot
3VT	41	12	6	59
ARSA	3	1	1	5
DCS	1	1	0	2
LVOT	30	9	4	43
HLHS	9	3	1	13
TGA	8	2	1	11
VSD	4	2	1	7
AVSD	4	2	1	7
ECIF	15	4	3	22
NH	55	16	8	79
Total	**170**	**52**	**26**	**248**

2.3. Data augmentation

Data augmentation is applied to increase dataset size [21]. The choice of the best image augmentation technique relies on the particular task being performed, dataset and model being used. The techniques such as flipping(horizontal/vertical): $I'(x,y) = I(W-x-1,y)$, rotation: $x' = xcos(\theta) - ysin(\theta)$ and $y' = xsin(\theta) + ycos(\theta)$ and cropping are used in deep learning for image augmentation. After exhaustive research and in-depth analysis, deterministic image augmentation and WGAN-GP are used in this research work.

2.3.1. Deterministic image augmentation

Deterministic image augmentation applies fixed, predefined transformations to images, ensuring consistent and reproducible results as shown in Table 2. In the image preprocessing pipeline, a comprehensive data augmentation strategy was implemented that evolved in two distinct phases to optimize model performance. The affine transformations were carefully calibrated to preserve the essential characteristics of the images. While introducing meaningful variations rotations were constrained within -30° to 30° to maintain feature orientation. Scaling operations were applied with factors between 0.8 and 1.2 to ensure realistic size variations and horizontal/vertical flips were implemented with a 50% probability to double the effective dataset size. Elastic transformations were particularly valuable as they simulated natural deformations by applying random displacement fields, creating realistic variations that could occur in real-world scenarios. To further enhance the model's reliability and reduce the risk of overfitting, the augmentation pipeline was expanded with additional sophisticated techniques. Controlled noise was introduced through salt and pepper injection, which helped the model become more resistant to image artifacts and sensor noise. The final layer of augmentation included random cropping and padding operations within ±10% of the original dimensions, effectively teaching the model to handle varying object scales and positions. Two levels of deterministic augmentation were carried out. With single level augmentation dataset size was increased from 248 to 552 and with second level augmentation it has increased to 3518. This approach significantly increased the size of training data while maintaining the semantic integrity of the images.

Table 2. Dataset summary for deterministic image augmentation

Single-level Augmentation					Bi-level Augmentation				
Class	Training	Testing	Validation	Tot	Class	Training	Testing	Validation	Tot
3VT	41	12	6	59	3VT	247	72	35	354
ARSA	38	12	5	55	ARSA	248	72	35	355
DCS	36	11	5	52	DCS	211	61	30	302
LVOT	30	9	4	43	LVOT	240	70	34	344
HLHS	36	11	5	52	HLHS	245	71	35	351
TGA	32	10	6	48	TGA	247	72	35	354
VSD	34	10	5	49	VSD	247	72	35	354
AVSD	34	10	5	49	AVSD	249	72	36	357
ECIF	46	14	6	66	ECIF	246	71	35	352
NH	55	16	8	79	NH	276	80	39	395
Total	**382**	**115**	**55**	**552**	**Total**	**2456**	**713**	**349**	**3518**

2.3.2. Wasserstein GAN with gradient penalty

Wasserstein GAN with Gradient Penalty (WGAN-GP) was used [22]–[24] to generate images conditioned on class labels. Generator uses random noise and class labels to produce class-specific images. The discriminator (critic) compares actual and generated images, using the Wasserstein loss with gradient penalty to assure Lipschitz continuity. During training, the model updates the discriminator and the generator alternately. The gradient penalty stabilizes training by penalizing gradients. The generator learns to produce high-quality, diversified images, while the discriminator develops its ability to tell the difference between real and fake. Both use a Wasserstein loss to optimize the generative process. Finally, class conditioning enables the creation of images that belong to specified classes and expanded the dataset to 4264 as shown in Table 3.

Table 3. Dataset after WGAN generating

Classes	Train	Test	Validation	Total
Normal Heart	545	154	76	775
Abnormal Heart	2442	698	349	3489
Total	**2987**	**852**	**425**	**4264**

2.4. The proposed healthcare architectural framework

In each implemented model, raw FECG images are annotated using an annotation tool (LabelMe) to highlight areas of interest. These labeled images undergo data augmentation to enhance the dataset. The images are segmented to isolate key regions using deep learning models.

2.4.1. ResNet-101 architecture

The ResNet-101 model in Figure 2, a deeper variant of ResNet [25], [26], is pre trained on ImageNet and fine-tuned on the segmented ultrasound dataset. The pipeline consists of four main stages with a total of 101 layers, including initial and final layers. Stage 2 has 3 residual blocks, contributing to 9 layers, while stage 3 includes 4 residual blocks, making up 12 layers. Stage 4 is the deepest with 23 residual blocks, totaling 69 layers, and stage 5 contains 3 residual blocks with 9 layers. Final layers include average pooling layer, flattening, and a fully connected layer (FC) for classification.

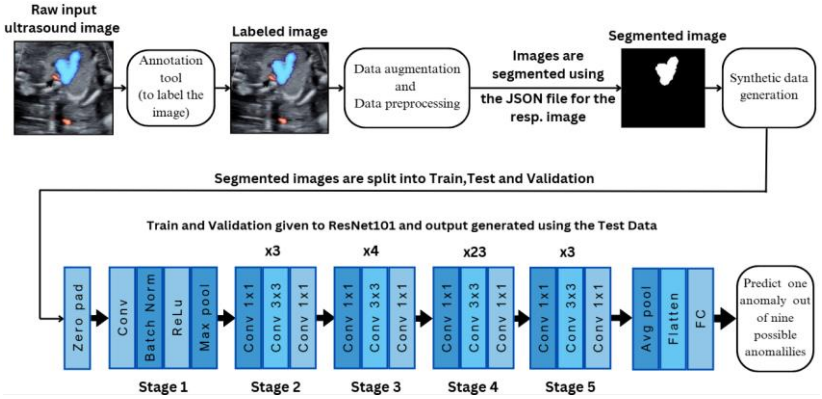

Figure 2. Proposed model with ResNet-101 architecture

2.4.2. WGAN-GP architecture

WGAN-GP is a stabilized GAN version that enhances training by introducing a gradient penalty for more consistent and authentic generation [27], [28]. The generator and critic compete in a minimax game. The critic aims to maximize the Wasserstein distance between real and generated images. The generator tries to minimize the distance to fool the critic. Gradient Penalty to enforce the Lipschitz constraint required by WGAN. A gradient penalty term is computed and added to the critic's loss function. The critic is updated multiple times per generator update to ensure strong feedback as shown in Figure 3. The generator $G(z)$ maps a random noise vector $z \sim p_z(z)$ to the data space. The generator's goal is to maximize the critic's estimation Wasserstein distance $maxE|z \sim p_z(z)[D(G(z))]|$.

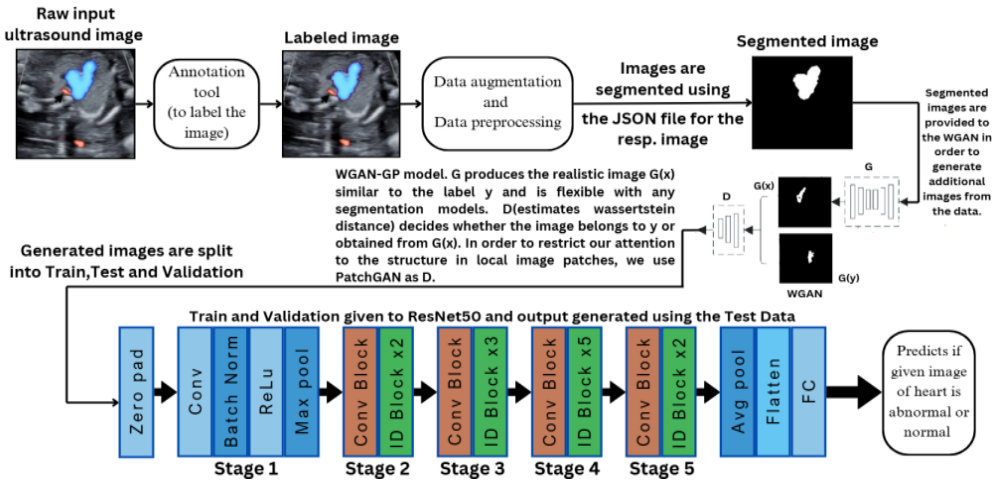

Figure 3. Proposed WGAN-GP with ResNet-50 architecture

2.4.3. Discriminator (critic) objective

Unlike traditional GANs, WGAN-GP does not use a sigmoid activation for the discriminator. Instead, it learns a function D(x) that estimates the Wasserstein distance between real and generated distributions. The critic's objective is

$$minEx\hat{}\sim p_g[D(x\hat{})] - Ex\hat{}\sim p_r[D(x)] + \lambda Ex\hat{}\sim p_x E[(\| \nabla_x \sim D(x\sim) \|_2 - 1)^2] \quad (4)$$

where $p_r(x)$ is the real data distribution. $P_g(x)$ is the generated data distribution. $x\sim$ is a linear interpolation between real and fake samples λ is the penalty coefficient. The gradient penalty term $E[(\| \nabla_x \sim D(x\sim) \|_2 - 1)^2]$ enforces the Lipschitz constraint by penalizing gradients to ensure stability during training.

3. RESULTS AND DISCUSSION

In this research, aim was to understand and examine fetal heart defects. The initial stride involved the procurement of a comprehensive dataset comprising fetal echocardiographic images which was curated to encapsulate diverse cardiac conditions. Employing domain expertise, various anomalies within the dataset were assigned appropriate nomenclature. Utilizing modern annotation techniques like LabelMe, areas of interest in the images are identified, establishing the way for segmentation. To improve diagnosis precision, the deterministic image augmentation and WGAN GP data augmentation method were used. Through segmentation, the images were categorized into distinct anatomical areas, each of which is crucial for identifying irregularities in the heart. Then, we utilized modern deep learning architectures. tailored to our dataset, ensuring optimal performance. According to the findings, which are summed up in the Table 4 data augmentation becomes crucial for enhancing model. We examined the various model's performances across a range of data sizes and augmentation methods including deterministic and WGAN for data enhancement. According to the findings, which are summed up in the Tables 4 and 5 data augmentation becomes crucial for enhancing model.

Table 4. Comparison of the models on deterministic augmented dataset

	Single-level Augmentation				Bi-level Augmentation		
Models	Accuracy	Precision	Specificity	Models	Accuracy	Precision	Specificity
ResNet-101	91.30	92.57	98.95	ResNet-101	99.15	99.16	99.91
ResNet-50	91.30	92.91	99.06	ResNet-50	96.49	96.75	99.60
DenseNet169	86.09	88.08	98.40	DenseNet169	92.99	93.55	99.19
VGG16	79.13	81.58	97.55	VGG16	82.47	83.30	98.02
EfficientNetB0	64.35	69.37	95.37	EfficientNetB0	71.53	72.85	96.84

3.1. Error metrics

Root mean square error (RMSE) is the metric used to measure the difference between true values and predicted values as shown in Figure 4, first image original image second one predicted value of image resulting from deterministic augmentation and last Image resulting from WGAN-GP.

$$RMSE = \sqrt{\frac{1}{n} \sum_{i=1}^{n} (yi - y\hat{})^2} \quad (5)$$

where $yi - True\ Value$, $y\hat{} - predicted\ value$ and n – Number of samples. For ResNet-101 model, the RMSE was found to be 0.0300 as shown in Table 5.

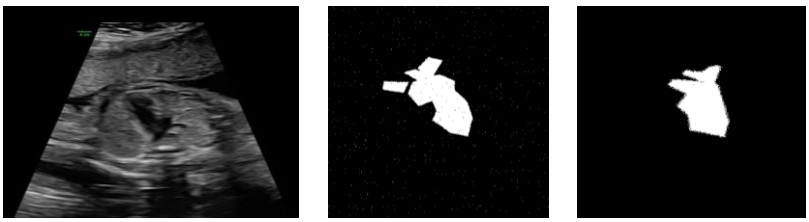

Figure 4. The difference between true values and the predicted values

Table 5. ResNet-101 Model performance

Augmentation	Accuracy	RMSE
Deterministic	99.15	0.0300
WGAN-GP	89.90	0.3075

The results and findings of earlier studies are compared. Table 6 shows that although deep learning methods are very successful in classifying, segmenting, and predicting complex medical images, the use of suitable augmentation techniques further improves model performance and greatly enhances accuracy.

Table 6. Comparison relation to data augmentation and fetal-safe imaging techniques

Ref	Classifier	Dataset	Performance matrix
[17]	GAN	The synthetic dataset is five times larger than the original data	Dice score achieved is 0.81, with a standard deviation of approximately 0.09
[14]	ResNet-50	The synthetic dataset increased by 13 times the size of the original dataset	Two datasets were used FETAL-125 and OB-125 Accuracy - 94.4% and 91.5% respectively
[29]	ResNet-50	Echocardiography	Around 75% accuracy
[18]	GAN-generated via IAGAN	The synthetic dataset increased by 9 times the size of the original dataset	Accuracy - 80% AUC - 0.90
[28]	ResNet-50 and Xception	The synthetic dataset increased by 3 times the size of the original data.	ResNet-50, Accuracy - 84.78% Xception Accuracy - 86.98%
Proposed work	ResNet-101	The two methods: i) Deterministic image augmentation techniques, ii) WGAN-GP expanded original datasets to 14 times and 17 times respectively.	Deterministic image augmentation Accuracy-99.15 WGAN-GP Accuracy-89.90

4. CONCLUSION

The data augmentation techniques can help us address the challenge of data scarcity and ensure that our system functions effectively across a range of patient demographics and clinical circumstances. Six out of nine classes achieved full performance accuracy using ResNet-101 with an average precision accuracy of 99.15%. The significance of this finding lies in the possibility of achieving high-quality outcomes with less data using two methods, deterministic image augmentation techniques and WGAN-GP. The results obtained have demonstrated superior performance compared to existing systems. The improvements in overall detection accuracy for fetal heart abnormalities have been validated by certified gynecologist and fetal medicine specialist confirming that our research approach outperforms traditional methods. Optimizing the proposed system for real-time deployment and seamless integration into existing clinical workflows is essential for its practical utility. Collaboration with healthcare institutions and industry stakeholders will be pivotal in developing user-friendly interfaces and interoperable systems. The limitation of this research is that images need to be labeled under expert guidance.

ACKNOWLEDGMENTS

Author wants to express my sincere gratitude to author's college and guide for providing the resources and support necessary for the completion of this research.

FUNDING INFORMATION:

Authors state no funding involved.

AUTHOR CONTRIBUTIONS STATEMENT

This journal uses the Contributor Roles Taxonomy (CRediT) to recognize individual author contributions, reduce authorship disputes, and facilitate collaboration.

Name of Author	C	M	So	Va	Fo	I	R	D	O	E	Vi	Su	P	Fu
Nusrat Jawed Iqbal Ansari	✓	✓	✓		✓	✓		✓	✓	✓	✓		✓	
Maniroja M. Edinburgh		✓				✓				✓	✓	✓		
Nikita				✓			✓	✓		✓	✓			

C : **C**onceptualization
M : **M**ethodology
So : **So**ftware
Va : **Va**lidation
Fo : **Fo**rmal analysis
I : **I**nvestigation
R : **R**esources
D : **D**ata Curation
O : Writing - **O**riginal Draft
E : Writing - Review & **E**diting
Vi : **Vi**sualization
Su : **Su**pervision
P : **P**roject administration
Fu : **Fu**nding acquisition

CONFLICT OF INTEREST STATEMENT

The authors report that no known competing financial interest or personal relationship appears to have influenced any of the work described in this paper.

INFORMED CONSENT

Informed consent was obtained from all participants involved in the study. They were fully informed about the study's purpose, procedures, and any potential risks before agreeing to participate.

DATA AVAILABILITY

The data that support the findings of this study are openly available in reference number [22].

REFERENCES

[1] L. J. Salomon *et al.*, "ISUOG Practice Guidelines (updated): performance of the routine mid-trimester fetal ultrasound scan," *Ultrasound in Obstetrics & Gynecology*, vol. 59, no. 6, pp. 840–856, Jun. 2022, doi: 10.1002/uog.24888.

[2] A. J. Moon-Grady *et al.*, "Guidelines and recommendations for performance of the fetal echocardiogram: an update from the American Society of Echocardiography," *Journal of the American Society of Echocardiography*, vol. 36, no. 7, pp. 679–723, Jul. 2023, doi: 10.1016/j.echo.2023.04.014.

[3] M. C. Fiorentino, F. P. Villani, M. Di Cosmo, E. Frontoni, and S. Moccia, "A review on deep-learning algorithms for fetal ultrasound-image analysis," *Medical Image Analysis*, vol. 83, p. 102629, Jan. 2023, doi: 10.1016/j.media.2022.102629.

[4] M. Komatsu *et al.*, "Detection of cardiac structural abnormalities in fetal ultrasound videos using deep learning," *Applied Sciences*, vol. 11, no. 1, p. 371, Jan. 2021, doi: 10.3390/app11010371.

[5] O. J. Benavidez, K. Gauvreau, and T. Geva, "Diagnostic errors in congenital echocardiography: importance of study conditions," *Journal of the American Society of Echocardiography*, vol. 27, no. 6, pp. 616–623, Jun. 2014, doi: 10.1016/j.echo.2014.03.001.

[6] S. Geman, E. Bienenstock, and R. Doursat, "Neural networks and the bias/variance dilemma," *Neural Computation*, vol. 4, no. 1, pp. 1–58, Jan. 1992, doi: 10.1162/neco.1992.4.1.1.

[7] S. Ioffe and C. Szegedy, "Batch normalization: accelerating deep network training by reducing internal covariate shift," *Preprint arXiv:1502.03167*, Mar. 2015.

[8] H.-C. Shin *et al.*, "Medical image synthesis for data augmentation and anonymization using generative adversarial networks," in *In Simulation and Synthesis in Medical Imaging: Third International Workshop, SASHIMI 2018*, 2018, pp. 1–11, doi: 10.1007/978-3-030-00536-8_1.

[9] S. Nurmaini *et al.*, "Deep learning-based computer-aided fetal echocardiography: application to heart standard view segmentation for congenital heart defects detection," *Sensors*, vol. 21, no. 23, p. 8007, Nov. 2021, doi: 10.3390/s21238007.

[10] S. Nurmaini *et al.*, "Deep learning for improving the effectiveness of routine prenatal screening for major congenital heart diseases," *Journal of Clinical Medicine*, vol. 11, no. 21, p. 6454, Oct. 2022, doi: 10.3390/jcm11216454.

[11] C. A. Combs, A. B. Hameed, A. M. Friedman, and I. A. Hoskins, "Special statement: Proposed quality metrics to assess accuracy of prenatal detection of congenital heart defects," *American Journal of Obstetrics and Gynecology*, vol. 222, no. 6, pp. B2--B9, Jun. 2020, doi: 10.1016/j.ajog.2020.02.040.

[12] R. Vullings, "Fetal electrocardiography and deep learning for prenatal detection of congenital heart disease," in *2019 Computing in Cardiology (CinC)*, Dec. 2019, pp. 1–4, doi: 10.22489/CinC.2019.072.

[13] C. Athalye and R. Arnaout, "Domain-guided data augmentation for deep learning on medical imaging," *PLOS ONE*, vol. 18, no. 3, p. e0282532, Mar. 2023, doi: 10.1371/journal.pone.0282532.

[14] E. Miskeen *et al.*, "Prospective applications of artificial intelligence in fetal medicine: a scoping review of recent updates," *International Journal of General Medicine*, vol. Volume 18, pp. 237–245, Jan. 2025, doi: 10.2147/IJGM.S490261.

[15] F. Nowak *et al.*, "An investigation into augmentation and preprocessing for optimising X-ray classification in limited datasets: a case study on necrotising enterocolitis," *International Journal of Computer Assisted Radiology and Surgery*, vol. 19, no. 6, pp. 1223–1231, Apr. 2024, doi: 10.1007/s11548-024-03107-0.

[16] H. M. Balaha, A. O. Shaban, E. M. El-Gendy, and M. M. Saafan, "A multi-variate heart disease optimization and recognition framework," *Neural Computing and Applications*, vol. 34, no. 18, pp. 15907–15944, Sep. 2022, doi: 10.1007/s00521-022-07241-1.

[17] C. Tiago *et al.*, "A data augmentation pipeline to generate synthetic labeled datasets of 3D echocardiography images using a GAN," *IEEE Access*, vol. 10, pp. 98803–98815, 2022, doi: 10.1109/ACCESS.2022.3207177.

[18] S. Motamed, P. Rogalla, and F. Khalvati, "Data augmentation using generative adversarial networks (GANs) for GAN-based detection of Pneumonia and COVID-19 in chest X-ray images," *Informatics in Medicine Unlocked*, vol. 27, p. 100779, 2021, doi: 10.1016/j.imu.2021.100779.

[19] X. Wang, K. Wang, and S. Lian, "A survey on face data augmentation for the training of deep neural networks," *Neural Computing and Applications*, vol. 32, no. 19, pp. 15503–15531, Oct. 2020, doi: 10.1007/s00521-020-04748-3.

[20] R. Stoean, D. Iliescu, C. Stoean, C. Patru, and R. Nagy, "Second trimester fetal echocardiography data set for image segmentation," *Figshare Figure*, 2022, doi: 10.6084/m9.figshare.21215597.

[21] Q. Ning and Z. Qi, "WGAN-GP_Glu: A semi-supervised model based on double generator-Wasserstein GAN with gradient penalty algorithm for glutarylation site identification," *Computers in Biology and Medicine*, vol. 184, p. 109328, Jan. 2025,

doi: 10.1016/j.compbiomed.2024.109328.
[22] G.-C. Lee, J.-H. Li, and Z.-Y. Li, "A Wasserstein generative adversarial network–gradient penalty-based model with imbalanced data enhancement for network intrusion detection," *Applied Sciences*, vol. 13, no. 14, p. 8132, Jul. 2023, doi: 10.3390/app13148132.
[23] C. Ng, "Generative adversarial network (generative artificial intelligence) in pediatric radiology: A systematic review," *Children*, vol. 10, no. 8, p. 1372, Aug. 2023, doi: 10.3390/children10081372.
[24] K. He, X. Zhang, S. Ren, and J. Sun, "Deep residual learning for image recognition," in *2016 IEEE Conference on Computer Vision and Pattern Recognition (CVPR)*, Jun. 2016, pp. 770–778, doi: 10.1109/CVPR.2016.90.
[25] M. F. Aslan, K. Sabanci, and A. Durdu, "A CNN-based novel solution for determining the survival status of heart failure patients with clinical record data: numeric to image," *Biomedical Signal Processing and Control*, vol. 68, p. 102716, Jul. 2021, doi: 10.1016/j.bspc.2021.102716.
[26] Y. Fu, M. Gong, G. Yang, H. Wei, and J. Zhou, "Evolutionary GAN–based data augmentation for cardiac magnetic resonance image," *Computers, Materials & Continua*, vol. 68, no. 1, pp. 1359–1374, 2021, doi: 10.32604/cmc.2021.016536.
[27] I. E. Tibermacine *et al.*, "Adversarial denoising of EEG signals: a comparative analysis of standard GAN and WGAN-GP approaches," *Frontiers in Human Neuroscience*, vol. 19, May 2025, doi: 10.3389/fnhum.2025.1583342.
[28] B. Zhang, H. Liu, H. Luo, and K. Li, "Automatic quality assessment for 2D fetal sonographic standard plane based on multitask learning," *Medicine*, vol. 100, no. 4, p. e24427, Jan. 2021, doi: 10.1097/MD.0000000000024427.
[29] Y. Gong *et al.*, "Fetal congenital heart disease echocardiogram screening based on DGACNN: adversarial one-class classification combined with video transfer learning," *IEEE Transactions on Medical Imaging*, vol. 39, no. 4, pp. 1206–1222, Apr. 2020, doi: 10.1109/TMI.2019.2946059.

BIOGRAPHIES OF AUTHORS

Nusrat Jawed Iqbal Ansari is currently pursuing a PhD degree in electronics and telecommunication engineering from the University of Mumbai, India. She is working as an assistant professor in the Department of Computer Engineering at Vivekanand Education Society's Institute of Technology, Chembur, India. Her research interests include signal processing, artificial intelligence, image processing and machine learning. She can be contacted at email: nusrat.ansari@ves.ac.in.

Maniroja M. Edinburgh holds a Ph.D. in electronics from SGBAU, Maharashtra, India. She is the Head of the Department of Electronics and Telecommunications Engineering at TSEC, Mumbai. She holds 31 years of work experience in academics and is a recognized Ph.D. Guide of the University of Mumbai. She has around 30 national/international journal publications, around 24 national/international conferences and received a minor research grant from the University of Mumbai. She can be contacted at email: maniroja@thadomal.org.

Nikita is Certified Gynecologist and Fetal Medicine Specialist, Gynecological Laparoscopic Surgeon (MUHS, FMAS, ICOG) assistant professor, Department of Obstetrics and Gynecology at P.G Medical Trust Hospital. Published extensively in national and international journals. Author of "Conception to Confinement". She can be contacted at email: drnikita1962@gmail.com.